HOW CONNECTED IS CONNECTED? STRUCTURAL MEASURES TO ESTIMATE EFFECTIVE CONDUCTIVITY

by

Jeffrey Klakovich

A Thesis Submitted to the Faculty of the

DEPARTMENT OF HYDROLOGY & ATMOSPHERIC SCIENCES

In Partial Fulfillment of the Requirements

For the Degree of

MASTER OF SCIENCE

WITH A MAJOR IN HYDROLOGY

In the Graduate College

THE UNIVERSITY OF ARIZONA

2018

STATEMENT BY AUTHOR

The thesis titled *How Connected is Connected? Structural Measures to Estimate Effective Conductivity* prepared by *Jeffrey Klakovich* has been submitted in partial fulfillment of requirements for a master's degree at the University of Arizona and is deposited in the University Library to be made available to borrowers under rules of the Library.

Brief quotations from this thesis are allowable without special permission, provided that an accurate acknowledgement of the source is made. Requests for permission for extended quotation from or reproduction of this manuscript in whole or in part may be granted by the head of the major department or the Dean of the Graduate College when in his or her judgment the proposed use of the material is in the interests of scholarship. In all other instances, however, permission must be obtained from the author.

SIGNED: *Jeffrey Klakovich*

APPROVAL BY THESIS DIRECTOR

This thesis has been approved on the date shown below:

April. 25th 2018

Ty P.A. Ferré
Professor of Hydrology &
Atmospheric Sciences

Date

ACKNOWLEDGEMENTS

Mom and Dad (for their endless love and support), Ben Paras (for helping me learn MATLAB), Chloé Fandel (for giving feedback and encouragement), Jesse Dickinson (for being an amazing resource), and Ty Ferré (for outstanding mentorship and fostering learning and discovery so well).

Funding for this project came in part from the University of Arizona Department of Hydrology & Atmospheric Sciences.

Table of Contents

List of Figures

Abstract

Connectivity has been a target of investigation for subsurface hydrology for decades. We apply seven new and existing connectivity measures to 2-D, binary hydraulic conductivity (K) grids that include a range of percent high K mixtures. Effective conductivity (K_{eff}) is calculated from the results of flow simulation (MODFLOW) and compared with connectivity measures. In addition, characteristics of the percolating network (connected high K bodies that span entire domain) are investigated. Results indicate that most of the range of K_{eff} (80%-90%) for approximately 1 million randomly generated grids over a range of percent high K mixtures only exists among percolating grids. We demonstrate that the number of unique percolating paths (NPP) is the most important structural feature for predicting K_{eff}. We show that NPP can explain to a large degree the mean behavior of K_{eff} as a function of percent high K material. It may also explain the variance of K_{eff} as a function of percent high K, however this has not been shown conclusively. Most connectivity measures were not found to correlate with K_{eff}. In general, it seems connectivity is only important for K_{eff} when high and low K values are similar (one order of magnitude different). Therefore, the overall impact of connectivity is relatively small. The dependence of K_{eff} on the continuity of high K paths suggests that methods that return volume-averaged properties (e.g. electrical resistivity tomography) may have limited ability to predict K_{eff}. High resolution imagery or water isotopic tracer tests to infer structure may be necessary for accurate estimation of K_{eff} at the field scale.

Introduction

Hydraulic conductivity (K) is a primary control on subsurface flow and, therefore, transport. At the sample scale, K depends on particle size distribution, sorting, and structure. Particle size distribution (PSD) is relatively easy to measure and forms the basis of most pedotransfer functions (Coppola et al., 2013; Schaap et al., 2001). There are few practical methods to measure soil structure, introducing considerable uncertainty which is often represented as dual porosity (Samardzioska and Popov, 2005), preferential flow (Logsdon, 2002), and PSD-mixture models (Dann et al., 2009). At larger scales, there is some promise of measuring important structures, especially using geophysical and tracer methods. Generally, these methods seek to identify organized bodies of high or low permeability. But, this relies on a fundamental assumption – that hydrologically important structures can be identified from images of soil structure. While this may be true for the simplest of structures, such as distinct beds, it is unclear which structural features constitute connected, conducting (or impeding) structures.

In this study, we examine the simplest conditions to test existing and propose new measures of connectivity that have relevance for water flow. Specifically, we consider two-dimensional structures experiencing a 1-D gradient under steady state conditions. Further, the media are binary: comprised of only two materials with relatively higher and lower hydraulic conductivity (K). Our motivating question is: given a perfect image of the K distribution, are there structural measures that can reliably predict the effective hydraulic conductivity (K_{eff}) of the medium?

Based on previous research, we expect that three characteristics will control effective conductivity. First, the relative abundance of high K material. Second, the structure of the high K regions. This may be defined based on basic geostatistical properties, such as correlation length, or on connectivity, which is the extent to which higher K materials are connected in space (Lee et al., 2007). Third, percolation, which describes the presence of connected high K pathways that extend entirely from one boundary to another in the direction of flow. The objective of this work is to examine the contributions of these elements to K_{eff}. Having done this, I will comment on the implications of these findings for our ability to use imaging techniques to improve estimation of K_{eff}.

VOLUME-WEIGHTED AVERAGING

The simplest methods of estimating effective hydraulic conductivity only consider the particle size distribution, and do not take structure into account. These methods calculate K_{eff} as the volume-weighted average of the hydraulic conductivities of materials. Usefully, there are two end member distributions that can be analyzed exactly. First, when the particles are organized into layers that are parallel to the applied gradient and second, when they are in series relative to the gradient. Parsons and Cardwell (1945) demonstrated that effective conductivity for any assemblage of materials lies between the K_{eff} of these two scenarios. Specifically, particle layers parallel to the applied gradient have K_{eff} equal to the volume-weighted arithmetic mean of the points of conductivity, whereas K_{eff} of series arrangement equals the volume-weighted harmonic mean. Futher, Matheron (1967) proved that an infinite system of heterogeneous conductivities having isotropic spatial correlation and lognormal frequency distribution has an effective conductivity equal to the geometric mean. But, others have concluded that there is no simple average that is valid for all heterogeneous formations (Wen and GomezHernandez, 1996). A power average method for

finding upscaled hydraulic conductivity has been applied in other studies (Desbarats, 1992; Deutsch, 1989). In this method, K_{eff} is calculated from the volume-weighted averages of the points of conductivity raised to an exponent. By varying the exponent between -1 and 1, the power average varies between the harmonic and arithmetic averages. Theoretically, the geometric average corresponds to the exponent set to zero (Wen and GomezHernandez, 1996).

CORRELATION LENGTH

Spatial variability of a heterogeneous K field can be described with geostatistical methods. A central concept in geostatistics is covariance, a measure of how much two variables change together. The correlation between two measurements separated by some distance is described by their spatial covariance. Generally, higher correlation is expected between points that are close to each other. Conversely, correlation decreases with increasing separation distance. At some scale, measurement values become practically uncorrelated with each other (Güngör-Demirci and Aksoy, 2011). This maximum distance is the correlation length; beyond this, values become spatially independent (Webster et al., 2007). Practically, the correlation length of a heterogeneous K field can indicate the average size and separation of high K (or low K) bodies. Correlation length typically is determined by sampling. With determined variance and correlation length of a sample population, K distribution on larger scales can be estimated using variograms, covariance models, or kriging. With inferred maps of K distribution, we can estimate effective, or upscaled, hydraulic conductivity. The underlying premise is that the structure, specifically the geostatistics of the structure, defines the effective properties. This is often used to generate multiple realizations of heterogeneous field with the assumption that fields with the same geostatistical properties will lead to comparable hydrologic responses.

Geostatistical techniques are powerful tools that work on limited data. They can be used to characterize any variable that can be measured, not just K. Entin et al. (2000), Western et al. (1998), and Western et al. (2004) used geostatistical methods to characterize spatial soil moisture patterns. Western et al. (2004) found that post-modeling data collection of soil moisture confirmed the accuracy of their variograms. "Variograms for these four patterns are similar which indicates that variograms used for the structural analysis are highly reliable" (Western et al., 1998). However, the accuracy of a given variable's "geostatistical correlation structure" (Western et al., 1998) is strongly subject to the sample correlation length, variance, and relative anisotropy. Güngör-Demirci (2011) considered several heterogeneous K fields with diverse correlation lengths to assess the impact of varying correlation length on optimal pump-and-treat remediation design. Their results showed that the size of low and high K zones defined by correlation length affected remediation design and cost noticeably (Güngör-Demirci and Aksoy, 2011). Thus, uncertainty about the representativeness of sample parameters is of high concern in geostatistical modeling.

Most applications of geostatistics are not well-suited to estimating upscaled hydraulic conductivity because they do not account for the contributions of geologic connectivity. As Western et al. (2001) pointed out, "Connectivity is a property that is not captured by standard geostatistical approaches which assume that spatial variation occurs in the most random possible way that is consistent with the spatial correlation." In their assessment of the impact of varying the K heterogeneity conditions on optimal pump-and-treat remediation designs, Güngör-Demirci (2011) found the specific locations of low and high K zones were particularly important for designing appropriate remediation efforts. They

concluded that better definition of the spatial distribution of K was needed than that provided by their geostatically-generated K fields (Güngör-Demirci and Aksoy, 2011).

CONNECTIVITY FUNCTION

The connectivity function is the prevalent geostatistical measure of geologic connectivity. Originally introduced by Allard (1994), the connectivity function $\tau(h)$ is defined as the lag-dependent probability that a point (x) is connected to another point (x+h) separated by a distance h (Western et al., 2001). It is determined by sampling all points in space. More recently, Western et al. (2001) introduced the integral connectivity scale, I_τ, representing the average distance over which any two points are connected (Western et al., 2001). Western et al. (2001) concluded that the connectivity function captures visually obvious connectivity quite well. They also show that, when using soil moisture as an indicator, the connectivity function can be correlated with surface runoff behavior (Western et al., 2001).

It has been shown that the connectivity function is not perfect. Knudby and Carrera (2005) drew different conclusions from their tests of the connectiviy function than that of Western et al. (2001). Knudby and Carrera (2005) state "it seems clear that … the ability of CS_4 [the connectivity function] to capture the connectivity difference is diminished by the presence of many small, above-threshold zones." In other words, Knudby and Carrera (2005) point out that the connectivity function will underestimate significant connectivity if there exist many small, disconnected high K zones in conjuction with connected pathways. Both studies conclude that the connectivity function has some value for predicting flow behavior (and, to a lesser extent, transport behavior). But, importantly, the connectivity function performs much better when applied only in the direction of regional (average) head gradient (Knudby and Carrera, 2005; Western et al., 2001).

SPATIAL ARRANGEMENT METRICS

Key structural features that may give rise to hydrologically-significant connectivity have been suggested, although not rigorously tested (Deutsch, 1998; Fogg et al., 2000; Lee et al., 2007). Fogg et al. (2000) introduce a stochastic model where primary aquifer units (comprising only 18% of the system) are 70% connected into one channel domain that fully percolates (interconnects) in all three dimensions. Demonstrated plausibility of the model led authors to consider specific features of high K channels, such as the maximum length in the x, y, and z directions (Fogg et al., 2000). Correlation between these features and system effective conductivity was not reported by Fogg et al. (2000), however metrics developed in the current study based on these descriptions seek to explore this relationship.

Deutsch (1998) introduced several measures of connectivity, and provided software tools for their calculation for 3D porosity and permeability models. Connectivity measures include the number, sizes, surface area, and tortuosity of high K clusters. Specific connectivity between two objects (i.e., percolation) is also considered, and a program for its identification is provided. Specifically, all of these programs are applicable to three-dimensional numerical geological models (Deutsch, 1998). But, again, the hydrological significance of these metrics was not explored.

PERCOLATION THEORY

A system with a continuous, spanning path is said to be percolating. Percolation has particular meaning for two end points that are joined by a percolating path, and may have important effects on the overall connectivity of the system. Conditions where percolation

can arise in random media are described by percolation theory, a branch of probability theory that defines threshold relationships in connectivity. The critical fraction, sometimes called the percolation threshold, is defined as the fraction of conducting portions at which the probability of percolation increases from 0 to 1 for an infinite rectangular grid (Hunt et al., 2014; Stauffer, 1985). For heterogenous K fields, this translates to the fraction of the media which is comprised of high K material. Lehmann (2007) and Berkowitz (1998) both report a percolation threshold of 0.6, or sixty percent, meaning that a subsurface system of infinite extent is guaranteed to have a unified channel of high K for the condition of 60% or greater high K.

This well-known rule of percolation theory is generally reflected in finite systems, too. For instance, Lehmann (2007) reported percolation occurring between 46.5% to 82.5% for random two-dimensional grids sized 50x20, with approximately half of all grids percolating at sixty percent. Thus, percolating and non-percolating realizations may exist above and below the percolation threshold for real systems. We define the percolation threshold at 60% high K material, which is coincident with half of all grids percolating.

Methods

Connectivity measures were tested in the simplest conditions: 2-D structures experiencing a 1-D gradient at steady state. 2-D was chosen for simplicity, believing 3-D to be overly-complex for a first-level analysis. Further, the media are binary, with only two materials of relatively higher and lower K. The size of the grid is 25 x 25, chosen for computational efficiency and to permit visual comparison. Effective conductivity, K_{eff}, was determined based on the results of a steady state flow model using MODFLOW. MODFLOW models were composed of 25 rows, 25 columns, and 1 layer. Every cell has length one and units are in centimeters. Given scalability, solutions would be identical in any length or time unit and would only require a change of one or two variables in the MODFLOW code to account for density and viscosity constants. The left and right sides of the model are constant head boundaries of 200 and 100, respectively. Top and bottom boundaries are no flow boundaries, so flow occurs left to right. Figure 1 is a sample grid showing constant head boundaries, no flow boundaries, and flow direction. K_{eff} was calculated with Darcy's Law using the MODFLOW flow result, as show in Equation 1.

Equation 1. Method of calculating K_{eff} from MODFLOW results. Q is total flow, 25 is the cross-sectional area of the model, 24 is the distance between constant head boundaries, and 100 is total change in head across the grid.

$$K_{eff} = \frac{Q}{A} * \frac{dL}{dH} \quad \longrightarrow \quad K_{eff} = \frac{Q}{25} * \frac{24}{100}$$

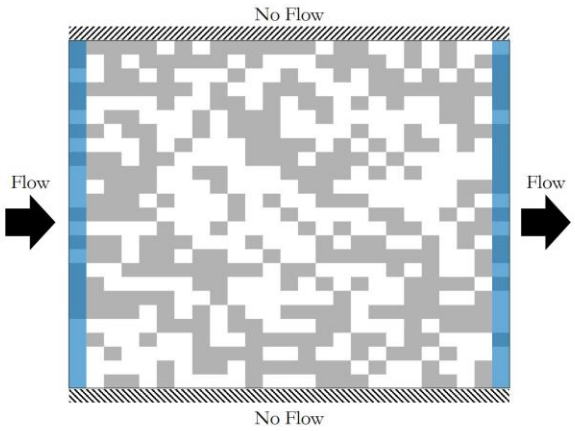

Figure 1. Sample K grid with high K (white) and low K (grey) cells, constant head boundaries (blue), no flow boundaries (diagonal lines) and flow direction (arrows). Area of the model is 25 x 25 x 1. The left boundary has a constant head of 200 and right boundary has a constant head of 100, with flow occurring left to right.

Ten thousand grids were randomly generated for every 1% high K condition from 1% to 99% high K, totaling in 990,000 grids. Grids were generated with the Matlab function *rand*, a pseudorandom number generator that creates uniformly distributed random numbers on the interval [0 1]. A fraction of these numbers (based on the percent high K condition) was replaced with the number one, and the rest were replaced with the low K value. Each grid was used in multiple flow simulations to consider three levels of high K/low K: 1/0.1, 1/0.01, and 1/0.001. Levels of K contrast are referred to as low contrast, medium contrast, and high contrast, respectively. As a result, each K contrast condition used exactly the same set of 990,000 grids, allowing for direct comparison among these cases.

Table 1. Connectivity metrics used in this study. C1 - C6 return only one value per grid. C7 returns a number for each cluster in one grid. C2 and C4 have several size thresholds.

Metric	Description
C1	*Length of longest high K cluster
C2	Number of high K clusters that span 20% grid length … 40% grid length … 60% grid length … 80% grid length … 100% grid length
C3	**Width of widest low K cluster
C4	Number of low K clusters that span 20% grid width … 40% grid width … 60% grid width … 80% grid width … 100% grid width
C5	Number of high K - high K connections parallel to flow
C6	Number of low K - low K connections perpendicular to flow
C7	***Clumpiness mean … standard deviation … variance … sum

* Length is measured parallel to flow.

** Width is measure perpendicular to flow.

*** Clumpiness equals cluster size divided by area of cluster's smallest bounding rectangle. Clumpiness statistics consider all the clusters in one grid.

Several new and existing connectivity metrics were tested on grids and compared against K_{eff} (Table 1). Most metrics examine features of high K or low K clusters. High K clusters were defined by 4-way connectivity, meaning that high K cells must be connected by their edges. This was chosen because the flow between any two cells takes place over the faces, requiring high K on both sides of a face to constitute a connected high K path. Conversely, low K clusters were defined by 8-way connectivity, and a group of low K cells connected by edges or corners constituted a cluster. In this case, two low K blocks connected by their corners effectively block any connected high K pathway through that cell. The Matlab function *bwlabel* identifies unique clusters in 2-D space by 4-way or 8-way connectivity, allowing for easy cluster analyses (Figure 2). C1-C4 measure the length and width of clusters. Given that flow no-flow boundaries are horizontal, a cluster's length is defined here as the horizontal distance from the leftmost edge to the rightmost edge of a cluster. Its width is the vertical distance from topmost edge to the bottommost edge. Alternatively, C5 and C6 count cell connections: high K – high K connections parallel to flow and low K – low K connections perpendicular to flow. These measure the directional organization of high K cells parallel to flow, and low K cells perpendicular to flow, respectively.

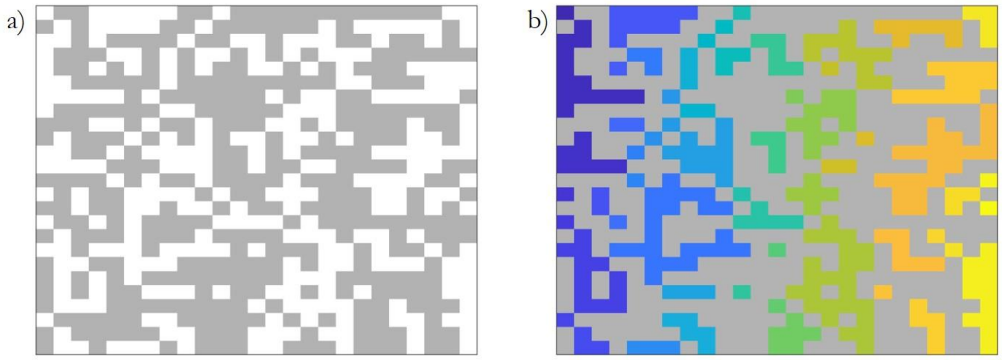

Figure 2. Identifying unique high K clusters with the Matlab function *bwlabel*. a) Binary grid with high K (white) and low K (grey). b) Binary grid with each high K cluster identified by 4-way (edge only) connectivity. Colors represent 57 unique clusters.

Flow paths that percolated the entire grid were analyzed in addition to testing connectivity metrics. A percolating path is defined as a continuous path of high K cells that connects both constant head boundaries. A percolating path may traverse the grid perpendicular to flow, but may not travel against the regional (average) head gradient. Similar to the definition of high K cluster, a percolating path is made of high K cells connected along their edges, not corners. Percolating paths were distinguished as follows. First, grids were translated into graph objects based upon the position of high K cells relative to each other. Graph objects are comprised of 'nodes' and 'edges', and high K cells were converted into nodes linked by edges of uniform length. A high K cell could be connected with up to three neighboring high K cells: to the left, to the right, and directly in front (i.e. "downstream"). Connections transverse to the flow direction permitted two-way flow, while connections parallel to flow allowed flow only in the down-gradient direction.

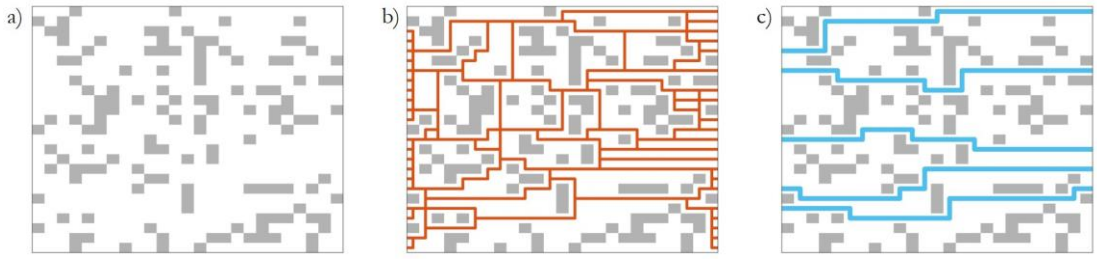

Figure 3. Process of determining the number of unique percolating paths, NPP. a) Sample grid. b) Sample grid with every possible percolating path between constant head boundaries identified. c) Sample grid with only unique percolating paths, showing NPP=5.

With each grid converted into a graph object, the Matlab function *shortestpath* was used to calculate the shortest percolating paths between boundary cells. To be sure to collect all possible percolating paths, the shortest path was identified between every combination of high K boundary cells (i.e., along the left and right edges of the grid). This produced a list of all possible percolating paths. Frequently, most percolating paths crossed each other (Figure

3b). From this list, the shortest unique percolating paths were selected by process of elimination. First, the shortest path was selected. All paths that crossed the shortest path were deleted from the list. This was repeated until the list comprised a unique list of percolating paths (Figure 3c). The number of paths on the final list is known as the number of *unique* percolating paths, or NPP.

Results

To begin analyzing all simulation results, a set of example grids was examined. This set has only five grids, each comprising 60% high K (Figure 4). The five grids include the theoretically highest permeability arrangement (perfect parallel, Figure 4f) and the theoretically lowest permeability arrangement (perfect series, Figure 4b). The three other grids have K material placed randomly. Using the method described above, K_{eff} was calculated for each grid and the three random grids were ordered from lower (Figure 4c) to higher (Figure 4e) permeability. The parallel and series K_{eff} values were calculated analytically for all percent high K (the results agreed, exactly, with the numerical approach). The shaded region on Figure 4a is bounded by these cases, indicating the range of achievable K_{eff} for any configuration. Grids e and f have the greatest difference in K_{eff}. There is very little difference in K_{eff} between grids b and c. Interestingly, grid e is percolating with three continuous high K paths (Figure 4e). But the sixteen high K paths of grid f (considering each row to be a separate percolating path) lead to much higher permeability. Following this change, there are small, but significant decreases in K_{eff} as the grids transition from many percolating paths (grid e) to a single percolating path (grid d), to no percolating paths (grid c). The differences in K_{eff} lead to a clustering of the random grids closer to that of perfect series arrangement than perfect parallel. Statistically, perfectly parallel and perfectly series are identically likely in randomly chosen grids. However, if this sample is representative, it is likely that relatively

lower K_{eff} grids are more common. The remainder of the results test these results across many random grids and to attempt to explain what controls K_{eff} in random binary grids.

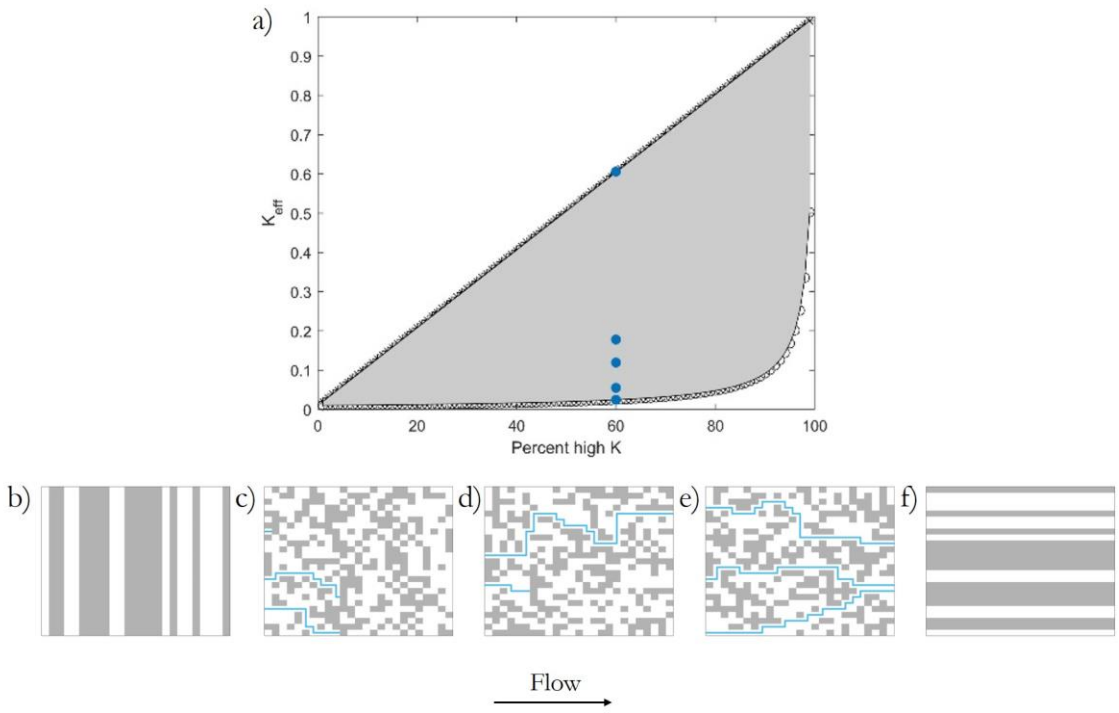

Figure 4. Five arrangements of 60% high K with different K_{eff}. a) Grids are plotted by their K_{eff}, where b<c<d<e<f. Shaded area indicates region of space within which K_{eff} could theoretically occur at any percent high K.

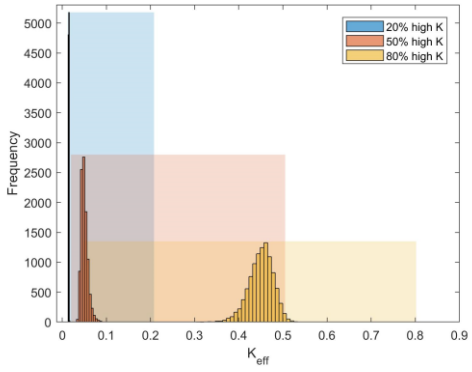

Figure 5. K_{eff} distributions (histograms) relative to limits (shaded areas) at 20%, 50%, and 80% high K at medium contrast.

To examine K_{eff} distribution among a larger sample of random grids, consider 10,000 random grids, each with one of three % high K conditions: 20% (blue), 50% (orange), and 80% (yellow). The frequency distribution of K_{eff} is shown for each condition on Figure 5. The shaded regions indicate the possible range of K_{eff} for each high K condition, extending from perfectly series to perfectly parallel cases. Distributions of K_{eff} at 20% and 50% high K

are biased toward the low end of the window of possible values and have low variance. This is consistent with findings of the example grids shown above. The 80% high K condition produces K_{eff} distribution with greater variance that is centered closer to the middle of the range of possible values. This suggests that the tendencies seen in the example grids apply for grids containing mostly low K material, but may not apply as high K becomes dominant.

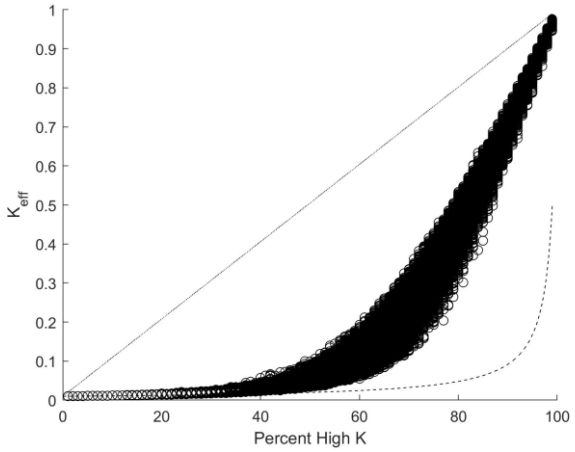

Figure 6. K_{eff} distribution as a function of percent high K for medium K contrast condition.

The analysis of the distribution of K_{eff} is extended to all percent high K values, with 10,000 values of K_{eff} for every 1% high K between 1% and 99% high K (see Figure 6). The dashed lines on Figure 6 indicate the limits of K_{eff} for each percent high K condition. The results for medium contrast case (i.e., high K=1, low K=0.01) are consistent with those shown above: differences will be discussed in more detail below. K_{eff} values are biased toward the lower limit. This bias is greater for lower percent high K conditions. The variance increases for higher percent K grids, but it decreases toward 100% high K. There is almost no change in K_{eff} below 40% high K. Then, there is a sharp, exponential rise in K_{eff} between 40% and 80% high K. Finally, there is a steep, linear increase in K_{eff} from 80% to 99% high K. Most of the change in K_{eff} occurs within this narrow, linear region. The middle, non-linear region between 40% and 80% high K has the greatest variance in K_{eff}.

The results for the high contrast grid are repeated for all three K contrasts in Figure 7. The high K value was held constant for the low contrast (yellow), medium contrast (orange), and high contrast (blue) cases. Because only the low K value was changed, the results differ most at 0% high K. There is a much greater difference between the low and medium contrast cases, even though the relative change in the low K value was the same between the low and medium and the medium and high. Figure 7a and Figure 7b show the same plot with two different plot orders because the degree of overlap between the medium and high contrast cases is so great. Similarities in the general shapes of the plots for the contrast

conditions suggest that similar factors may be controlling K_{eff}, but that the exact contrast in K values influences specific behavior.

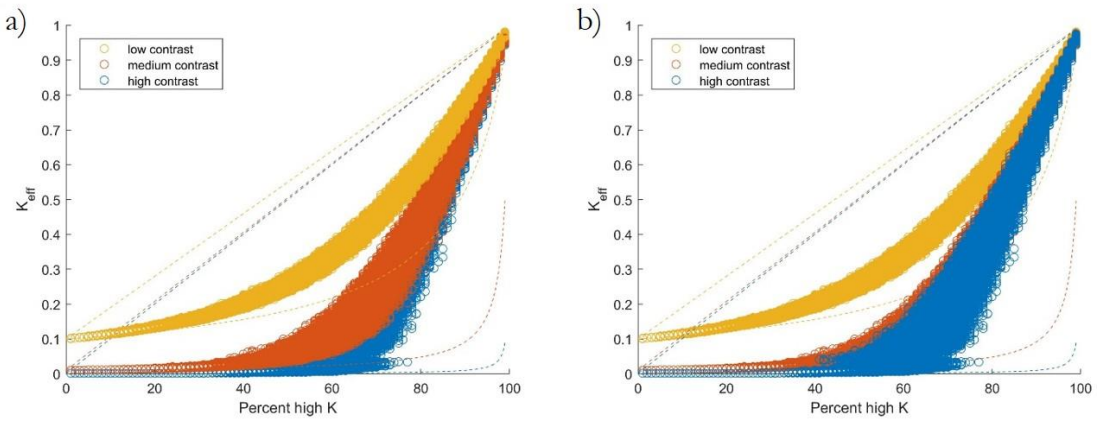

Figure 7. K_{eff} distributions across all percent high K using three K contrasts: low (yellow), medium (orange), and high (blue). Dashed lines are K_{eff} limits. a) High over medium over low. b) low over medium over high.

The medium and high contrast cases are highly similar. But, there are some differences in the shape of the low contrast results. In particular, the variance is lower and more consistent across percent high K values. Second, the exponential rise in K_{eff} is roughly constant from low percent high K to high percent high K, rather than showing a pronounced bend seen at higher contrast cases. This may indicate that the volume average of materials, and not connectivity or percolation of high K, governs K_{eff} at low contrast. Therefore, we will first address high and medium contrast while considering connectivity and percolation, and will revisit low contrast afterwards.

Our first attempt to explain the calculated K_{eff} results sought to correlate seven structural metrics with K_{eff}. These metrics rely on analyzing the connectivity of high K materials in the direction of flow, or the connectivity of low K transverse to flow. All but two metrics showed no statistically significant correlation with K_{eff}. Two metrics did correlate with K_{eff} (i.e., C5 and C6). But, these metrics also correlate with percent high K, and appear not to increase the accuracy of a prediction of K_{eff} provided by the volume ratio alone. Figure 8 shows the results of three connectivity metrics plotted against K_{eff} at medium contrast. Both C5 (Figure 8b) and C6 (Figure 8a) resemble K_{eff} distribution by percent high K (Figures 6 and 7), except that C5 is shifted to the left and C5 is the mirror image shifted to the right. Results from C7 mean (i.e. mean clumpiness) is shown in Figure 8c. As for the C7 mean, the other connectivity metrics listed in Table 1 show very low correlation. This surprising result suggests that efforts to quantify connectivity may have little value for hydrologic flow studies: the best connectivity metric used here is no more explanatory than a simple measure of soil texture.

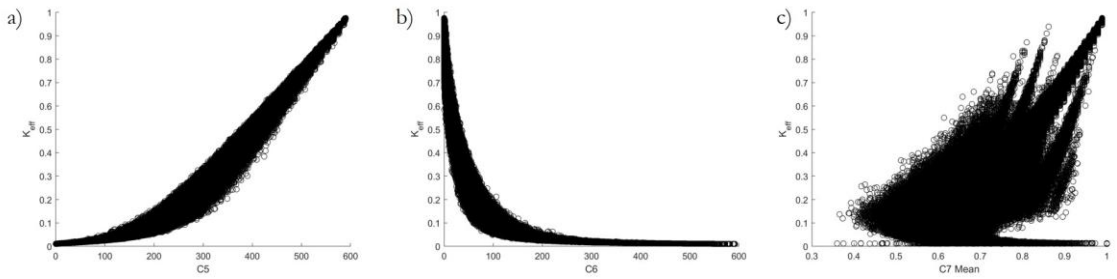

Figure 8. Three connectivity metrics plotted against K_{eff}. a) C6. b) C5. c) C7 Mean or mean clumpiness. C5 and C6 are the only metrics that show any correlation with K_{eff}.

Having failed to demonstrate that structural connectivity could explain K_{eff}, the examination extended to considering percolation. Figure 9 shows the percent of grids that are percolating at each percent high K. The first percolating grid appears at 41% high K. Percolating grids do not exceed 1% of all grids until 50% high K. At 60% high K, approximately half of all grids are percolating. The last non-percolating grid is seen at 77% high K. The region from 41%-77% high K is defined here as the percolation zone. The 60% percolation threshold in our results was also reported for an infinite rectangular grid by Lehmann (2007) and Berkowitz (1998). Lehmann (2007) also report similar upper and lower limits for the percolation zone for two-dimensional grids sized 20 x 50.

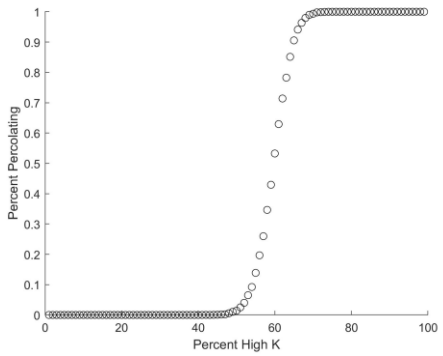

Figure 9. Transition from non-percolating to percolating with increasing percent high K. Approximately half of grids are percolating at 60% high K.

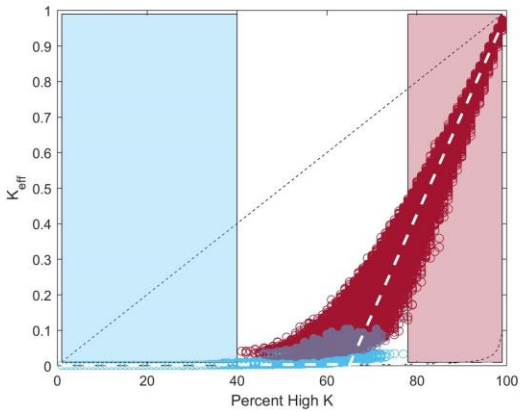

Figure 10. K_{eff} distribution at medium contrast showing percolating fields (red) and non-percolating fields (blue). Near-linear distributions of K_{eff} below 40% high K (blue shaded region) and above 78% high K (red shaded region) are approximated by dashed lines

The upper and lower limits of the percolation zone separate percent high K into three regions, defined here as zone 1 (lowest K_{eff}), zone 2 (intermediate K_{eff}), and zone 3 (highest K_{eff}). These zones are shown as color-shaded regions in Figure 10. The K_{eff} distribution shows the highest variance within zone 2. The mean response at each % high K varies approximately linearly in zones 1 and 3; the linear trends are shown as dashed lines in Figure 10. Slopes and y-intercepts of the trend lines are given in Table 2. In general, the linearity in these regions may suggest a simple relationship between K_{eff} and a volume average of specific K materials. In zone 1, the slope of the mean K_{eff} at any given % high K versus the % high K for medium and high contrast differ by approximately the same amount as the slopes of the series cases in these regions (one order of magnitude). This correlation agrees with previous findings of strong bias of K_{eff} toward the harmonic mean at lower percent high K. Conversely, slopes in zone 3 are similar for medium and high contrast cases. This suggests that the conductivity of the low K material is less important to the mean trend of K_{eff} in zone 3. Rather, some characteristics of the grid structure may govern flow behavior at higher percent K.

Table 2. Linear estimates of K_{eff} as a function of percent high K in zones 1 and 3 at both medium and high contrast. Lines are described according to slope-intercept form, *y= mx+b*.

	m		b	
	Zone 1	Zone 3	Zone 1	Zone 3
Medium Contrast	0.000467	0.0268	0.01	-1.7
High Contrast	5.38E-05	0.0282	0.001	-1.83

Both the trend of K_{eff} with percent high K and the variance of K_{eff} at each percent high K differ within the three zones. The variance is approximately normally distributed as a function of percent high K (Figure 11). As expected, the variance of K_{eff} variance is high for higher contrasts. The peak variance occurs near 70% for all contrast conditions. Interestingly, 99% of all grids are percolating above 70% high K, indicating most variance occurs among percolating grids.

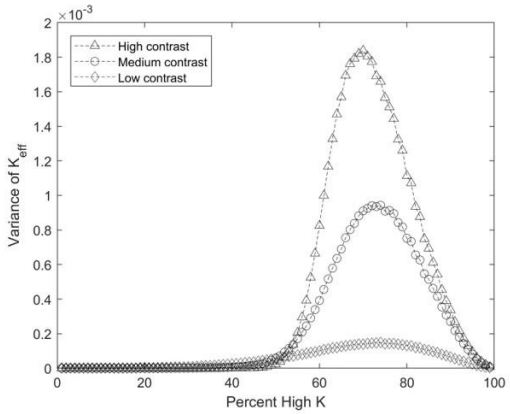

Figure 11. Variance of K_{eff} for every percent high K for high (triangles), medium (circles), and low (diamonds) contrast.

The example grids indicated that the largest absolute change in K_{eff} was due to the number of percolating paths (NPP). Examining all of the grids, NPP is found to correlate well with K_{eff} (see Figure 12a). On average, grids with one percolating path have higher K_{eff} than non-percolating grids; additional percolating paths have an additive effect on K_{eff}. The additive effect is non-linear: maximum K_{eff} increases 0.5 with the first 5 percolating paths, and only 0.2 with an additional 5 paths. Unlike connectivity metrics, NPP is correlated with K_{eff} independent of the percent high K condition. Figure 12b shows the relationship between NPP and K_{eff} at medium contrast for 70% high K. At this volume ratio, anywhere between 0 and 5 percolating paths may exist, and each additional path correlates with an increase in the mean K_{eff} for each NPP level.

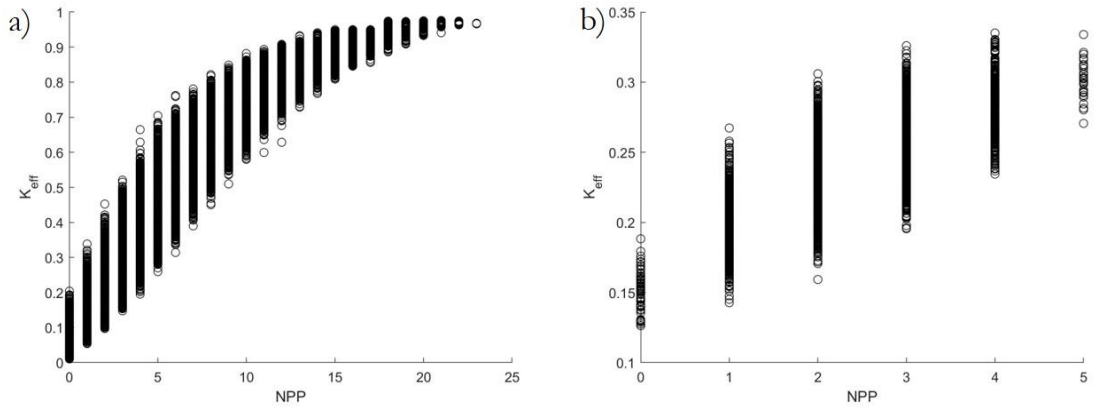

Figure 12. Relationship between number of percolating paths (NPP) and K_{eff}. a) K_{eff} plotted against NPP for all grids. b) K_{eff} plotted against NPP for only 70% high K grids.

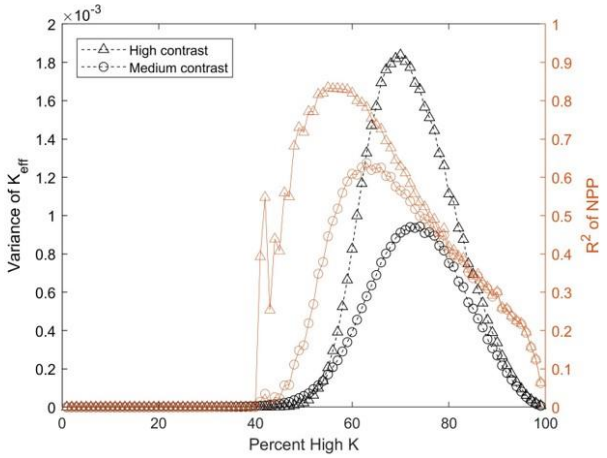

Figure 13. NPP as a predictor of K_{eff} for given percent high K conditions. a) K_{eff} plotted against NPP for 70% high K grids. b) K_{eff} variance and R^2 of NPP by percent high K.

NPP is a better predictor of K_{eff} for higher K contrast conditions (Figure 13). But, NPP does not explain all of the observed variance of K_{eff}. Intuitively, the lower permeability of the low K material used to form the high K contrast condition leads to greater importance of any high K paths. This should lead to a stronger correlation between NPP and K_{eff} for the higher contrast condition. In fact, the largest R^2 value for NPP does increase from medium contrast (0.6374) to high contrast (0.8339) (Figure 13). NPP has maximum correlation with K_{eff} around 60% high K. At this range, 47% of grids are non-percolating, 47% are percolating with 1 path, and 6% are percolating with 2 paths. Above 60% high K, correlation of NPP with K_{eff} decreases (Figure 13). This supports the suggestion made by Figure 4 that the first several percolating paths are most significant for flow; changes in K_{eff} diminish with further increases in NPP. Maximum variance of K_{eff} occurs near 70% when most grids have between 1 and 5 percolating paths. This further indicates the controlling influence of the first few percolating paths. However, an R^2 of 0.535 at 74% high K suggest that something(s) other than NPP – e.g. the length or tortuosity of the first few percolating paths – play an equal or greater part in controlling the variance of K_{eff}.

Discussion

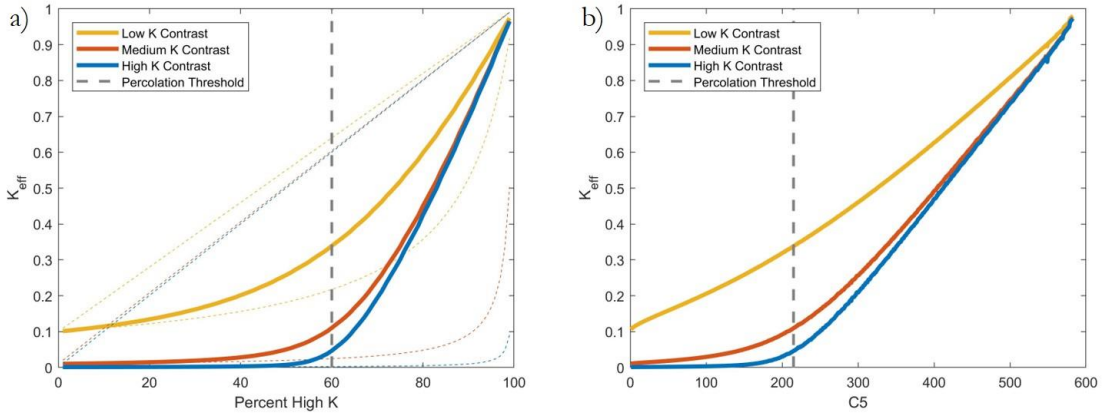

Figure 14. Distribution of mean K_{eff} for low (yellow), medium (orange), and high (blue) contrast conditions. Grey, dashed vertical line is the percolation threshold. a) K_{eff} as a function of percent high K. b) K_{eff} as a function of connectivity.

In general, K_{eff} distribution as a function of percent high K is biased toward the case of perfect series for all K contrast conditions. The mean K_{eff} for each contrast condition is plotted with upper and lower K_{eff} limits (i.e. K_{eff} of perfect parallel and perfect series cases) as dashed lines of the same color on Figure 14. More specifically, mean K_{eff} is biased toward the series case for low percent high K, but tends toward the average of the parallel and series cases as percent high K increases. Notably, each contrast condition produces a different distribution. The mean K_{eff} curve at low contrast (yellow) curves upward with a steadily increasing slope with increasing percent high K. Conversely, the high contrast (blue) curve comprises two semi-linear sections joined by an abrupt transition, marked with a grey, dashed vertical line (Figure 14a). This transition occurs 60% high K, the percolation threshold, defined here as the percent high K condition above which more than half of all grids are percolating. The medium (orange) contrast condition falls between these two curve types. For medium and high contrast, the percolation threshold marks the percent high K condition below which mean K_{eff} increases relatively little, and above which K_{eff} increases linearly with a steep slope. Mean K_{eff} for low K contrast shows no distinct change at the percolation threshold (Figure 14a).

Figure 14b shows mean K_{eff} for low contrast (yellow), medium contrast (orange), and high contrast (blue) as a function of connectivity (i.e. C5). Connectivity correlates strongly with percent high K, and thus, K_{eff} as a function of connectivity (Figure 14b) and a function of percent high K (Figure 14) look similar. The grey, dashed line in Figure 14b is the same percolation threshold as that in Figure 14a – for 60% high K condition, most grids have C5=215, so the two thresholds are nearly equivalent. Although Figure 14a and b share similarities, they differ most notably for low K contrast condition. In particular, the distribution of mean K_{eff} for low contrast is nearly linear and the slope does not change much as a function of percent high K. This may indicate that connectivity provides a more direct control on K_{eff} for low K contrast conditions. For medium and high contrast conditions, there appears to be two near-linear sections, joined around the percolation threshold. This difference between low and medium/high contrast conditions may be an indication of different roles for low K regions under these conditions. For higher contrasts,

a few obstructions along a high K path can greatly impede flow. For lower contrasts, flow 'around' obstructions may be comparable to flow along high K pathways.

Strong similarities between mean K_{eff} as a function of percent high K (Figure 14a) and as a function of connectivity (Figure 14b) for both medium and high K contrast show that connectivity is not a dominant force for K_{eff} for higher K contrast conditions. Effectively, both figures show two linear sections joined by a change in slope around the percolation threshold.

However, close examination shows that the linear sections of mean K_{eff} distribution are slightly more linear as a function of connectivity than as a function of percent high K. By way of explanation, imagine linear estimates imposed over the two linear sections (above and below the percolation threshold) of mean K_{eff} distribution for medium contrast (orange) both on Figure 14a and b. These linear fits are more accurate predictors of mean K_{eff} as a function of connectivity (Figure 14b) than as a function of percent high K (Figure 14a). In particular, they improve upon estimation of K_{eff} near the percolation threshold.

Considering that K contrast is only one order of magnitude different between low and medium contrast, it makes sense that well-connected – but discontinuous – paths may still conduct flow to some extent. Further, it makes sense that the weak effects of connectivity would be observed around the percolation threshold, where many grids are in 'near-percolating', and high connectivity indicates that many near-percolating paths may be present.

But, overall, connectivity has low influence over K_{eff} at medium contrast. At high K contrast, the influence of connectivity is indiscernible. This also makes sense: connected high K paths that are blocked by one low K cell conduct flow similar to that of other paths with many low K cells if the contrast is sufficiently high. Correspondingly, mean K_{eff} distribution as a function of percent high K (blue line on Figure 14a) has an abrupt change in slope with very little curve. The small section of curve that does exist lies between 50% and 70% high K – where percolating grids transition from 1% of total grids to 99% of total grids. This indicates that, for higher K contrast conditions, the influence of connectivity is completely overshadowed by percolation, possibly moderated by other aspects of percolating paths.

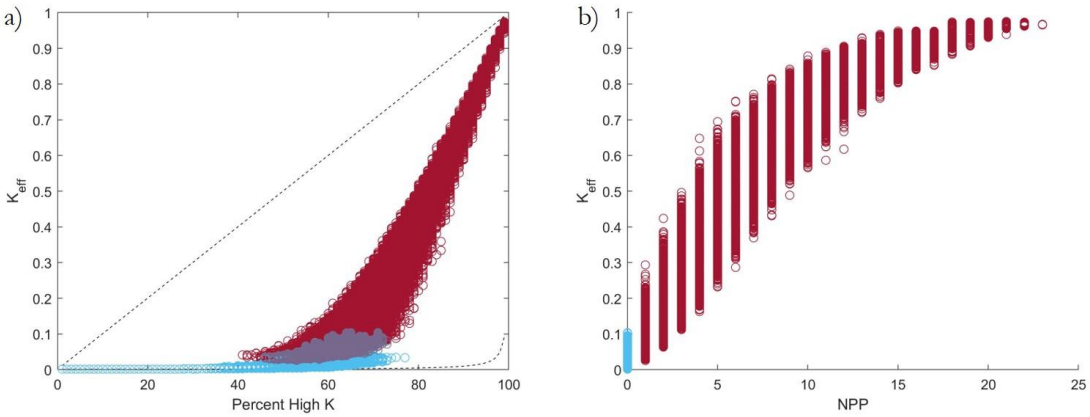

Figure 15. Distribution of K_{eff} for high contrast condition showing percolating (red) and non-percolating (blue) grids. a) K_{eff} as a function of percent high K. b) K_{eff} as a function of NPP, where non-percolating grids have NPP=0.

The percolation threshold marks the beginning of a steep rise in the distribution of K_{eff} as a function of percent high K (Figure 15a). K_{eff} of percolating (red) and non-percolating (blue) grids are shown for every percent high K condition in Figure 15a. Dashed lines in Figure 15a are the limits of possible K_{eff} for high contrast condition. We see that, although high K_{eff} is predicated on percolation, many percolating grids have low K_{eff} (Figure 15a). The lowest percent high K condition where percolation occurs is 41%, and K_{eff} shows very little change between 1% and 40% high K. K_{eff} of percolating grids from 40% to 50% high K increase incrementally. At 60% high K (the percolation threshold), half of all grids are percolating, and there is a wide range of K_{eff}. Generally, the grids with the highest K_{eff} are percolating while lower K_{eff} values are associated with non-percolating grids. But, some non-percolating grids have higher K_{eff} than some percolating grids (Figure 15a). Above the percolation threshold (>60% high K), the range of K_{eff} for any percent high K condition gets larger. The range of K_{eff} of non-percolating grids is narrow in comparison to the range seen for percolating grids. Around 75% high K marks the beginning of a near-linearly distributed increase in K_{eff} as a function of percent high K. As average K_{eff} increases, the range of K_{eff} gradually narrows for every percent high K condition, until minimum and maximum K_{eff} converge at 100% high K.

Increasing K_{eff} above the percolation threshold is highly correlated with the number of unique percolating paths (NPP). Figure 15b shows K_{eff} of percolating (red) and non-percolating (blue) grids as a function of NPP for high K contrast condition. K_{eff} of all non-percolating grids are represented as having NPP=0. By increasing NPP from 0 to 1, maximum K_{eff} increases by a factor of 3, minimum K_{eff} changes relatively little, and the range of K_{eff} more than doubles. This is the largest change in maximum K_{eff} seen for any single-step change in NPP (Figure 15b). This reinforces the idea that, while the percolation is important for higher K_{eff}, percolating grids may still have low K_{eff}. Addition of a second percolating path has a similar effect of increasing maximum K_{eff} by almost double. K_{eff} range increases slightly also. (Figure 15b). This trend continues with a gradual lessening of K_{eff} response for each single-step change in NPP. By NPP=5, K_{eff} ranges between 22% and 70% of the high K value. Increasing NPP above 5 has a noticeable diminishing impact on K_{eff}. Above NPP=8, maximum K_{eff} changes little between single-step changes in K_{eff}, but minimum K_{eff} increases more than that seen for lower values of NPP. Consequently, range of K_{eff} decreases at higher NPP.

The distribution of K_{eff} as a function of NPP indicates that, overall, NPP is the most important structural feature for predicting K_{eff}. A wide range of K_{eff} for any given NPP suggests that other, unidentified features impact K_{eff} as well. These may include structural characteristics relating to connectivity or to percolation, including tortuosity of percolating paths or number of convergent percolating paths. NPP indicates that the first 1-5 percolating paths are in the most impactful on K_{eff}, evidenced by a large increase in K_{eff} on average. Specifics about these paths may be particularly important. NPP also suggests that adding more unique percolating paths has a diminishing impact on K_{eff} at higher NPP. This reveals an important aspect about NPP. Namely, the range of NPP increases for higher percent high K grids. This is because NPP is more sensitive to the placement of low K cells at higher percent high K. For example, consider a homogeneous high K grid (NPP=25). Adding five low K cells would decrease NPP to 20 if low K cells were located along different flow paths; 24 if they were located along the same flow path. Thus, there are 4 possible NPP values for random grids with 5 low K cells. But the range of K_{eff} is low for random grids with 5 low K cells. This should help to explain the sloping shape of Figure

15b, and the low range of K_{eff} between 15 and 25 NPP. At this range, NPP is a poor predictor of K_{eff}.

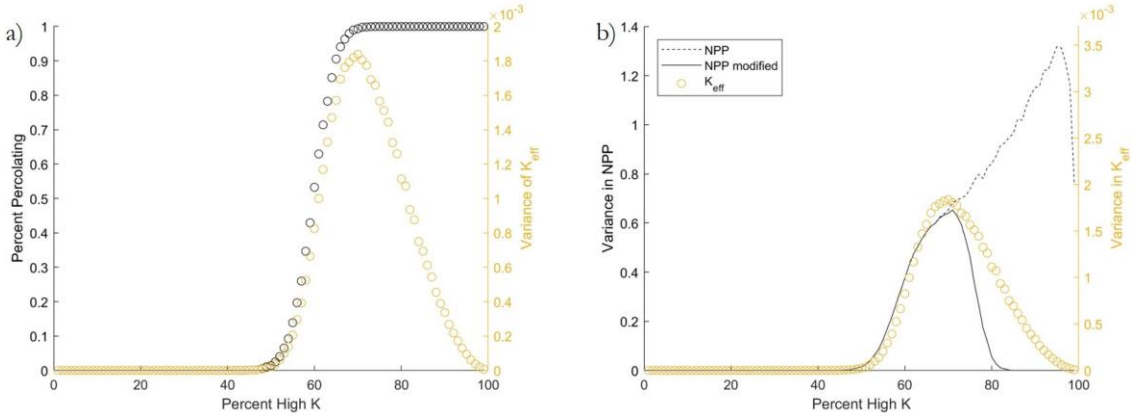

Figure 16. Variance in K_{eff} as a function of percent high K compared with percent of percolating grids and variance in NPP. a) Variance in K_{eff} and the percent of grids that are percolating as a function of percent high K. b) Variance in K_{eff} and variance in NPP as a function of percent high K. The dashed line is the true variance of NPP. The solid line is the variance in NPP if all NPP>4 are set equal to four.

Figure 16a shows both the total number of grids that are percolating and the variance in K_{eff} for high K contrast as a function of percent high K. Variance in K_{eff} is relatively low for less than 50% high K condition, reaching its highest around 70% high K. The number of possible grid configurations at any given percent high K is highest at 50% high K; it decreases sharply with increasing or decreasing percent high K. But, interestingly, the variance in K_{eff} does not follow this pattern. In fact, the increase in variance in K_{eff} as a function of percent high K closely mirrors the increase in relative number of percolating grids (a), indicating that variance in K_{eff} is controlled by grid structure rather than range of possible grid configurations. Percolating grids make up less than 1% of grids below fifty percent high K (Figure 16a). Between 50% and 60% high K, percolating grids increase from one percent to fifty percent of all grids. At seventy percent high K, 99% of grids are percolating. Thus, increasing variance in K_{eff} from 50% to 70% high K is highly correlated with the increasing prevalence of percolation.

One key finding of this work is that it is not the simple presence or absence of percolation that controls K_{eff}; it is the number of percolating paths. If the presence or absence of percolation controlled K_{eff} as a function of percent high K directly, we would expect the greatest variance in K_{eff} to occur at 60% high K, when half of grids are percolating. However, variance in K_{eff} peaks at seventy percent. Given the important role of NPP, we might expect that variance in K_{eff} is related to variance in NPP. Figure 16b shows that variance in NPP increases between 50% and 70% high K, bearing strong resemblance to variance in K_{eff} as a function of percent high K. However, unlike variance in K_{eff}, variance in NPP continues to increase from 70% to 99% high K (dashed line, Figure 16b). As discussed previously, NPP has a larger range at high percent high K; the dashed line on Figure 16b shows that NPP has greater variance at high percent high K as well.

The relationship between NPP and mean K_{eff} (Figure 15b) suggests that multiple percolating paths may have diminishing returns on K_{eff} at high NPP. To isolate the impact of the first 4 percolating paths on variance in K_{eff}, variance in NPP was calculated a second

time after setting all NPP>4 equal to 4. Variance of this modified NPP is the solid black line on Figure 16b. Variance of modified NPP approaches zero around 80% high K (i.e., most grids have NPP greater than or equal to four). Thus, the decrease in modified NPP variance does not resemble the decrease in variance in K_{eff}. But, this interesting result may suggest that, in addition to controlling mean K_{eff} distribution, variance in the number of percolating paths when NPP is low could also explain a large degree of variance in K_{eff}. Further, this figure suggests that some function of NPP that accounts for the diminished contribution of multiple percolating paths (rather than 'capping' NPP at 4, as modified NPP does) could have a variance curve that resembles variance in K_{eff}. If this were the case, the number of percolating paths would be a candidate for the primary control on mean and variance behaviors of K_{eff} as a function of percent high K. This points to the non-linear, additive effect of multiple percolating paths as an important topic that warrants further research.

Conclusions

The objective of this thesis was to understand the underlying, structural mechanisms that control the effective K of binary, random media over a range of percent high K mixtures. Conclusions can be made in two areas: on the dependence of the mean and the variance in K_{eff} as a function of percent high K. In general, there are two regimes of K_{eff} as a function of high K material: 1) less than 50% high K, which is controlled by connectivity, and 2) greater than 50% high K, controlled by percolation, especially the number of percolating paths. Both the mean and variance behaviors can be understood to be different in these two regimes.

The change in mean K_{eff} with change in % high K is steeper in regime 2 than in regime 1. In fact, ninety percent of the total K_{eff} range occurs within regime 2 (for high contrast; 80% for low contrast). This suggests that overall, NPP is the most important structural feature for predicting K_{eff}. The difference in this slope between regimes 1 and 2 is greater for higher K contrasts. This is largely due to a considerably smaller slope in regime 1 for high contrast conditions because of the dominance of lower K materials in series, which is more pronounced for a higher contrast. As the contrast decreases, the transition is smoother, more curved, suggesting that both connectivity and NPP are contributing to the dependence of K_{eff} on % high K in the zone of transition between the two regimes (approximately 40%-60% high). In conclusion, although connectivity has been a target of investigation for hydrologic studies for decades, it appears that its overall impact is relatively small and generally limited to relatively low percent high K conditions with relatively low K contrasts.

The variance in K_{eff} for a given percent high K is greatest when there is a more equal mixture of low and high K materials. That is, it peaks at larger percent high K in regime 1 and for lower percent high K in regime 2. By definition, the variance is zero at 0% and 100% high K because only one domain can be drawn for each of these cases. In fact, the number of possible grids as a function of percent high K peaks at 50% and drops sharply with increasing or decreasing percent high K. In regime 1, the number of different patterns that can be formed increases for increasing percent high K. As stated above, K_{eff} in regime 1 depends strongly on connectivity, which depends on the specific arrangement of high K cells. Therefore, on a simple geometric basis, it is expected that the variance in K_{eff} should increase with increasing percent high K. Although variance in K_{eff} in regime 1 follows this pattern, it does not reflect the exponential increase in possible grid configurations and

possible degrees of connectivity. Both appear to have little bearing on K_{eff} in regime 1. It is not until regime 2, with the increasing prevalence of percolation, that K_{eff} of random grids begins to vary greatly. Specifically, from 50% to 70% high K, there is a strong increase in variance with increasing percent high K, rather than a decrease consistent with the decreasing number of possible grids. Given that K_{eff} is due largely to percolation in regime 2, we could propose two drivers for variance: the presence or absence of percolation among grids at any % high K; or the variance of NPP at any given % high K. If the presence or absence of percolation controlled variance, we would expect the maximum variance to occur at the percent high K associated with 50% percolating grids: the widely accepted 60% high K percolation threshold. In fact, the peak variance in regime 2 occurs at 70% high K. Given that NPP was found to be more important than the simple presence/absence of percolation for explaining the mean K_{eff}, we might expect that the variance in K_{eff} across grids at a given percent high K would depend on the variance of NPP as a function of % high K. There appears to be a strong relationship between the variance of NPP and the variance of K_{eff} for percent high K ranging from 50-70%, but the variance in NPP continues to increase beyond 70%, whereas the variance of K_{eff} decreases beyond this point. By recalculating variance in NPP for only the first 4 percolating paths, and counting NPP>4 as being equal to 4, we see a variance that greater resembles variance in K_{eff}. That is, variance in this modified NPP reaches its maximum around 70% high K and decreases to zero around eighty percent high K. This curve shows better agreement with variance in K_{eff}. This suggests that some function of NPP that accounts for the diminished contribution of multiple percolating paths could have a variance curve that resembles variance in K_{eff}. If so, the number of percolating paths may explain variance in K_{eff} as well as mean behavior of K_{eff} as a function of percent high K.

In summary, we offer a nearly complete explanation of the underlying, structural mechanisms that control the mean and variance of Keff of binary, random media over the entire range of percent high K mixtures. We offer two possible explanations for the final piece: the reduction of the variance of K_{eff} above 70% high K. Although we tested previously suggested mechanisms that controls K_{eff}, and developed several new metrics, there is always the possibility that some other characteristic of random grids that we have not identified explains the variance for high percent high K conditions. This could include characteristics of percolating paths themselves, such as tortuosity, or some metric that considers the reduced impact of converging (non-unique) percolating paths. Or, the number of percolating pathways is responsible for variance in K_{eff}, but a direct measure of the number of percolating paths presented in this study doesn't fully capture this relationship because the contribution of multiple percolating paths diminishes when more percolating paths are present.

The findings of this research may have significance for flow and transport studies that aim to improve our ability to characterize effective, or upscaled, hydraulic conductivities. First, the results suggest that methods that are able to return volume averaged properties (e.g. electrical resistivity tomography) may have limited ability to predict K_{eff}, which depends on the continuity of high K paths. This suggest that high resolution imagery may be necessary to relate structure to K_{eff}. Second, measurements of K_{eff} may be very sensitive to the scale and orientation of tests. That is, while connectivity may be well described by geostatistical measures that apply at any location in a field, such as correlation length, percolation applies a higher threshold of continuous pathways spanning a domain. Therefore, as the measurement scale increases, or if the details of the connected pathways change with direction, the number of percolating paths may change. As shown, this may have a relatively large impact of the measured K_{eff}. Finally, the dependence of K_{eff} on NPP

may give weight to the use of water isotopic tracers for K estimation, as these may be more sensitive to advective transport through percolating pathways. Each of these topics is worthy of further research.

References

Allard, D., 1994, SIMULATING A GEOLOGICAL LITHOFACIES WITH RESPECT TO CONNECTIVITY INFORMATION USING THE TRUNCATED GAUSSIAN MODEL: Geostatistical Simulations: Proceedings of the Geostatistical Simulation Workshop, v. 7, p. 197-211.

Berkowitz, B., and R. P. Ewing, 1998, Percolation Theory and Network Modeling Applications in Soil Physics: Surveys in Geophysics, v. 19, p. 23-72.

Coppola, A., G. Dragonetti, A. Comegna, N. Lamaddalena, B. Caushi, M. A. Haikal, and A. Basile, 2013, Measuring and modeling water content in stony soils: Soil and Tillage Research, v. 128, p. 9-22.

Dann, R., M. Close, M. Flintoft, R. Hector, H. Barlow, S. Thomas, and G. Francis, 2009, Characterization and Estimation of Hydraulic Properties in an Alluvial Gravel Vadose Zone: Vadose Zone Journal, v. 8, p. 651.

Desbarats, A. J., 1992, Spatial averaging of hydraulic conductivity in three-dimensional heterogeneous porous media: Mathematical Geology, v. 24, p. 249-267.

Deutsch, C., 1989, Calculating Effective Absolute Permeability in Sandstone/Shale Sequences, v. 4, 343-348 p.

Deutsch, C. V., 1998, Fortran programs for calculating connectivity of three-dimensional numerical models and for ranking multiple realizations: Computers & Geosciences, v. 24, p. 69-76.

Entin, J. K., A. Robock, K. Y. Vinnikov, S. E. Hollinger, S. X. Liu, and A. Namkhai, 2000, Temporal and spatial scales of observed soil moisture variations in the extratropics: JOURNAL OF GEOPHYSICAL RESEARCH-ATMOSPHERES, v. 105, p. 11865-11877.

Fogg, G. E., S. F. Carle, and C. Green, 2000, Connected-network paradigm for the alluvial aquifer system: Theory, Modeling, and Field Investigation in Hydrogeology: a Special Volume in Honor of Shlomo P. Neuman's 60th Birthday, p. 25-42.

Güngör-Demirci, G., and A. Aksoy, 2011, Change in optimal pump-and-treat remediation design and cost for different correlation lengths of spatially variable hydraulic conductivity field: Quarterly Journal of Engineering Geology and Hydrogeology, v. 44, p. 469-480.

Hunt, A. G., R. P. Ewing, and B. Ghanbarian, 2014, Percolation theory for flow in porous media, v. 880.;880;: Cham, Springer.

Knudby, C., and J. Carrera, 2005, On the relationship between indicators of geostatistical, flow and transport connectivity: Advances in Water Resources, v. 28, p. 405-421.

Lee, S. Y., S. F. Carle, and G. E. Fogg, 2007, Geologic heterogeneity and a comparison of two geostatistical models: Sequential Gaussian and transition probability-based geostatistical simulation: Advances in Water Resources, v. 30, p. 1914-1932.

Lehmann, P., C. Hinz, G. McGrath, H. J. Tromp-van Meerveld, and J. J. McDonnell, 2007, Rainfall threshold for hillslope outflow: an emergent property of flow pathway connectivity: Hydrology and Earth System Sciences, v. 11, p. 1047-1063.

Logsdon, S. D., 2002, Determination of Preferential Flow Model Parameters: Soil Science Society of America Journal, v. 66, p. 1095.

Matheron, G., 1967, Élèments pour une théorie des milieux poreux: France U6 - ctx_ver=Z39.88-2004&ctx_enc=info%3Aofi%2Fenc%3AUTF-8&rfr_id=info%3Asid%2Fsummon.serialssolutions.com&rft_val_fmt=info%3Aofi%2Ffmt%3Akev%3Amtx%3Abook&rft.genre=book&rft.title=%C3%89l%C3%A8ments+pour+une+th%C3%A9orie+des+milieux+poreux&rft.au=Matheron%2C+G&rft.date=1967&rft.ext

ernalDBID=n%2Fa&rft.externalDocID=mdp.39015005871788&paramdict=en-US U7 - Book.
Parsons, R. L., and W. T. Cardwell, Average Permeabilities of Heterogeneous Oil Sands, p. 34-42.
Renard, P., and D. Allard, 2013, Connectivity metrics for subsurface flow and transport: Advances in Water Resources, v. 51, p. 168-196.
Samardzioska, T., and V. Popov, 2005, Numerical comparison of the equivalent continuum, non-homogeneous and dual porosity models for flow and transport in fractured porous media: Advances in Water Resources, v. 28, p. 235-255.
Schaap, M. G., F. J. Leij, and M. T. van Genuchten, 2001, rosetta: a computer program for estimating soil hydraulic parameters with hierarchical pedotransfer functions: Journal of Hydrology, v. 251, p. 163-176.
Stauffer, D., 1985, Introduction to percolation theory: London;Philadelphia;, Taylor & Francis.
Webster, R., M. A. Oliver, I. NetLibrary, and I. Wiley, 2007, Geostatistics for environmental scientists: Chichester;Hoboken, NJ;, Wiley.
Wen, X. H., and J. J. GomezHernandez, 1996, Upscaling hydraulic conductivities in heterogeneous media: An overview: JOURNAL OF HYDROLOGY, v. 183, p. R9-R32.
Western, A. W., G. Bloschl, and R. B. Grayson, 2001, Toward capturing hydrologically significant connectivity in spatial patterns: Water Resources Research, v. 37, p. 83-97.
Western, A. W., G. Blöschl, and R. B. Grayson, 1998, Geostatistical characterisation of soil moisture patterns in the Tarrawarra catchment: Journal of Hydrology, v. 205, p. 20-37.
Western, A. W., S.-L. Zhou, R. B. Grayson, T. A. McMahon, G. Blöschl, and D. J. Wilson, 2004, Spatial correlation of soil moisture in small catchments and its relationship to dominant spatial hydrological processes: Journal of Hydrology, v. 286, p. 113-134.